AN INVESTIGATION ON WINDMILL PALM LEAF SHEATH FIBER POWDER-BASED ACTIVATED CARBON FOR DYE ADSORPTION

Jiali Li
MD Student
E-mail: lijiali278237316@sina.cn

*Tonghua Zhang**
Professor
E-mail: zhtonghua@aliyun.com

Lan Cheng
PhD Student
E-mail: chenglan1437@sina.cn

Min Guo
PhD Student
E-mail: yiyaxida@126.com

Shu Wang
MD Student
E-mail: wangshu732@sina.com

Ruilong Ran
College of Textiles and Garments, Southwest University
Chongqing Engineering Research Center of Biomaterial Fiber and Modern Textile
Chongqing 400715, People's Republic of China
E-mail: 466325160@qq.com

Yifa Ma
Honghe Palm Industry Association
Yunnan 654400, People's Republic of China
E-mail: hhhhmyf@126.com

(Received August 2015)

Abstract. Windmill palm leaf sheath fiber (WPF) is an abundant agricultural byproduct and useful resource. To increase its valuable qualities and usefulness, we proposed to prepare WPF powder-based activated carbon (WPFAC) as a novel adsorbent for adsorbing methylene blue, with the specific aims for pollution treatment. The porous features of WPFAC were assessed based on nitrogen adsorption, and the adsorption capacity was studied by investigating the effect parameters of contact time, initial concentration, pH, and temperature. Research results showed a combination microporous and mesoporous structure of WPFAC with Brunauer–Emmett–Teller surface of 1049.26 m^2/g. WPFAC exhibited excellent adsorbing performance, and the maximum monolayer adsorption capacity was up to 51.78 times higher than other absorbents. Meanwhile, the adsorption capacity increased accordingly as the parameters increased. For better understanding, the adsorption behavior, isotherms, kinetics, and thermodynamics were studied using the equilibrium data. Investigation results illustrated that the equilibrium data were well consistent with the Langmuir isotherm, with a maximum monolayer adsorption capacity of 253.16, 289.85, and 303.95 mg/g

* Corresponding author

Wood and Fiber Science, 48(3), 2016, pp. 143-155

at 30°C, 40°C, and 50°C, respectively. The adsorption kinetics followed the pseudo-second-order kinetic model. Thermodynamic parameters: standard enthalpy ($\triangle H^0$), standard entropy ($\triangle S^0$), and standard free energy ($\triangle G^0$) indicated an endothermic and spontaneous absorbing process. WPFAC is a promising material that has high utility values for its amazing adsorption capacity.

Keywords: Windmill palm leaf sheath fiber, activated carbon, methylene blue, adsorption isotherm, kinetics, thermodynamics.

INTRODUCTION

The wastewater produced by the textile and other industries is currently one of the most important environmental issues in the world (Hameed et al 2009). Dye wastewater generally contains multifarious organic compounds and toxic substances, which may seriously pollute the environment and do harm to human beings (Liu et al 2015). In recent years, a variety of technologies, such as physicochemical, chemical, and biological methods, have been applied to treat dye effluents and have had obvious effectiveness (Vieira et al 2012). Meanwhile, new methods and techniques are constantly emerging in dye wastewater treatment agencies.

Amid various treatment approaches, adsorption is one of the most effective physical methods for removing dyes from textile effluents. Activated carbon is a commonly used adsorbent because of its capability to adsorb a broad range of adsorbates efficiently and its easy accessibility (Ahmad et al 2007). Nevertheless, commercially available activated carbons are subject to application limit because of high cost and unsatisfied absorption efficiency (Martin et al 2003). Hence, recently, attention has been focused on developing a low-cost adsorbent for the application of wastewater treatment. Studies include the use of orange peels, *Prunus domestica*, and *Jacaranda mimosifolia*, cellulose-based organogel, kenaf natural fibers, oil palm fiber (Tan et al 2007; Macías-García et al 2012; Maatar et al 2013; Treviño-Cordero et al 2013; Fernandez et al 2014).

Palm, which is widely distributed and a significant agricultural natural resource, is famed for its ornamental, greening, and economic advantages (Guo et al 2014). The development and use of windmill palm have received increasing attention. In our previous study (Cheng et al 2014), we studied the structural characteristics of windmill palm leaf sheath fiber (WPF). Results showed that WPF is a multicellular fiber and it exhibits porous features in the cross section. This structural feature may make WPF a potential candidate for filter and adsorption materials. However, as of yet, no relative investigation has been reported.

For rational development and effective use of natural resources, we propose to prepare WPF powder-based activated carbon (WPFAC) as a novel adsorbent with the specific aim of pollution treatment. In this study, we prepared WPFAC and evaluated the adsorption characteristics for methylene blue (MB) dye in simulation wastewater. Batch experiments were conducted to investigate the adsorption effects in terms of contact time, initial MB concentration (50-600 mg/L), solution pH (2-12), and temperature (30-50°C). To better understand the adsorption mechanism, experimental data of the adsorption were used to study adsorption isotherms, kinetics, and thermodynamics.

MATERIALS AND METHODS

Materials

Nowadays, MB is commonly used in the textile industry and becomes one of the major sources of wastewater pollutants. Therefore, we chose MB as the targeted adsorbate in this work. Its chemical formula is $C_{16}H_{18}ClN_3S$. Cationic dye MB was purchased from Coron Chemical Industry (Shanghai, China) without any purification treatment prior to use. Potassium hydroxide used as activating agent and hydrochloric acid and sodium hydroxide used for pH adjustment were all obtained from Coron Chemical Industry. Deionized water supplied by USF ELGA water

treatment system (Beijing, China) was used to prepare all reagents and solutions. MB and other reagents used in this work were all analytical grade reagents.

Windmill Palm Sheath Fiber Powder-Based Activated Carbon Preparation

The WPF used in this study was obtained from Honghe County, Yunnan Province, China. Dried WPF was powdered to particles with average size of 200 μm and loaded in a quartz tube reactor placed in a tube furnace. The WPF powder was then heated at a rate of 10°C/min from room temperature to 400°C and was maintained for 2 h under purified nitrogen (99.995%) flow. The char produced was mixed with water and KOH with an impregnation ratio of 1:2 for 0.5 h at 40°C and then dehydrated in an oven at 105°C. The dried mixture was activated under the same conditions as the carbonization step with similar heating rate and gas flow rate but to a final temperature of 850°C, which was held for 1 h. The resulting activated carbon was washed thoroughly to remove any impurities. HCl (1 M) solution was used to adjust the washing solution pH until it reached 6-8. After filtration, the remainder was dried at 60°C for 24 h.

Windmill Palm Sheath Fiber Powder-Based Activated Carbon Characterization

The Brunauer–Emmett–Teller (BET) surface area and pore size distribution were estimated using the standard nitrogen adsorption isotherm obtained by Micromeritics ASAP 2020 (Micromeritics Instrument Corporation, Norcross, GA).

Adsorption Experiments and Analytic Methods

Adsorption experiments were conducted in a set of 250-mL Erlenmeyer flasks containing 0.20 g adsorbent and 200 mL MB solutions with various initial concentrations (50, 100, 200, 300, 400, 500, and 600 mg/L). The sealed flasks were placed in an isothermal water-bath shaker and were shaken at 125 rpm at 30°C, 40°C, and 50°C and natural pH. At different time intervals, an aliquot of supernatant was withdrawn for analysis. The effect of pH was investigated at 40°C and an initial concentration of 200 mg/L, and pH adjustments were conducted using solutions of 0.1 M NaOH and 0.1 M HCl. The final concentration of the dye in the solution was measured at maximum wavelengths of MB (668 nm) using a visible spectrophotometer (721-VS, Shanghai Precision and Scientific Instrument Co., Ltd, Shanghai, China). The amount of equilibrium adsorption q_e (mg/g) on WPFAC was calculated with Eq 1:

$$q_e = \frac{(C_0 - C_e)V}{W} \quad (1)$$

where C_0 and C_e (mg/L) are the liquid-phase concentrations of the dye at initial and equilibrium, respectively; V is the volume of the solution (L); W is the weight of the adsorbent (g).

At predetermined time interval, the aqueous samples were taken and the dye concentrations were measured. The amount of adsorption at time t, q_t (mg/g), was calculated as follows:

$$q_t = \frac{(C_0 - C_t)V}{W} \quad (2)$$

where C_0 and C_t (mg/L) are the liquid-phase concentrations of the dye at the initial time and any time t, respectively.

The adsorption isotherms, kinetics, and thermodynamics were studied on the basis of experimental data.

RESULTS AND DISCUSSION

Windmill Palm Sheath Fiber Powder-Based Activated Carbon Characterization

Nitrogen adsorption is a standard procedure to determine the porosity of carbonaceous adsorbents (Foo and Hameed 2011), and the adsorption isotherm can provide qualitative information on the adsorption process and the extent of surface area available to the adsorbate (Brunauer et al 1938). Figure 1 shows the nitrogen adsorption isotherms of WPFAC. It indicated that the

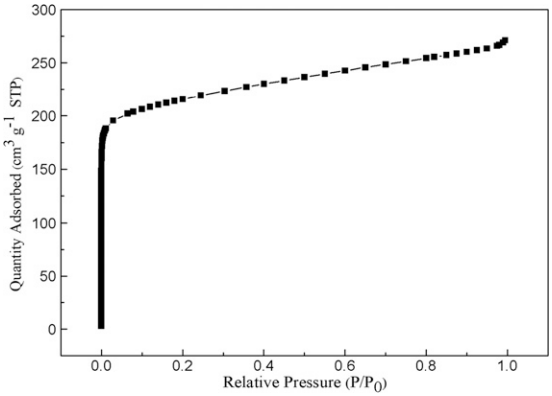

Figure 1. Nitrogen isotherm of windmill palm sheath fiber powder-based activated carbon.

isotherm of WPFAC corresponded to the intermediate between types I and II under the IUPAC classification, which was associated with a combination of microporous and mesoporous structures (Zhang et al 2015a). The BET surface area (1049.26 m^2/g) of WPFAC was markedly improved compared with that of the raw fiber (20.88 m^2/g), thereby implying the development of additional pores in the activated carbon.

Figure 2 shows the pore size distribution of WPFAC. The result revealed a sharp peak at a pore diameter of 1.7-50 nm, with an average pore size of 25.09 Å. A vast majority of pores fell within the range of 2-10 nm, in accordance with the presence of mesopore structure.

Effects of Contact Time and Initial Concentration on Adsorption

Figure 3 shows the adsorption amount vs the adsorption time at various initial MB concentrations at 30°C. For MB solutions with the initial concentrations of 50-200 mg/L, contact time of absorption is 0.5-2 h to reach equilibrium. For MB solutions with initial concentrations of 300-600 mg/L, an equilibrium time of 5-10 h was required. Results also showed that the MB adsorption was fast at the beginning and then became slower near the equilibrium. This phenomenon was caused by the fact that a large number of vacant surface sites were available for adsorption during the initial stage; after a certain time, the remaining vacant surface sites were difficult to occupy because of the repulsive forces between the solute molecules on the solid and bulk phases (Tan et al 2009). The amount of MB adsorbed onto the activated carbon increased with time and reached a constant value. At this point, a dynamic equilibrium process of MB adsorption onto and desorption off the WPFAC was formed. According to experimental data, the adsorption capacity at equilibrium (q_e) increased from 50 to 247 mg/g with an increase in the initial dye concentrations from 50 to 600 mg/L. This was caused by the fact that the initial concentration provided an important driving force to overcome all of the mass transfer resistances of the dye between the aqueous solution and solid phases. Therefore, a high

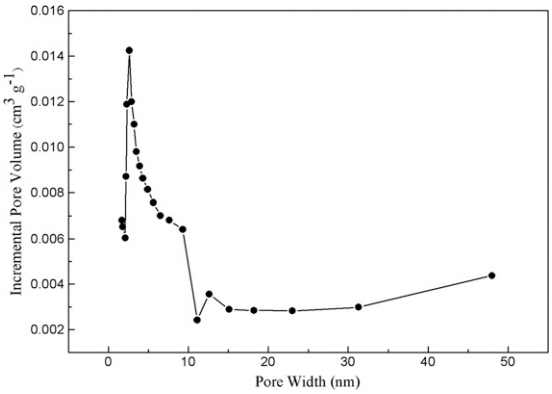

Figure 2. Pore size distribution of windmill palm sheath fiber powder-based activated carbon.

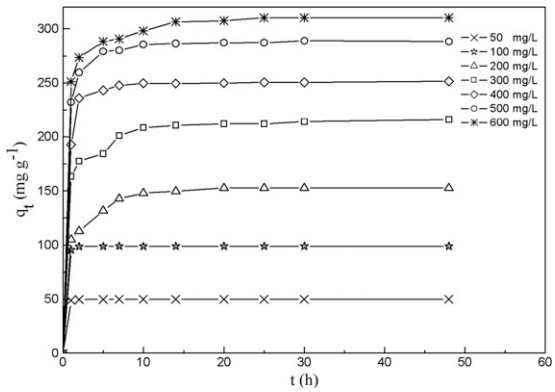

Figure 3. The variation of adsorption capacity with adsorption time at various initial methylene blue concentrations at 30°C.

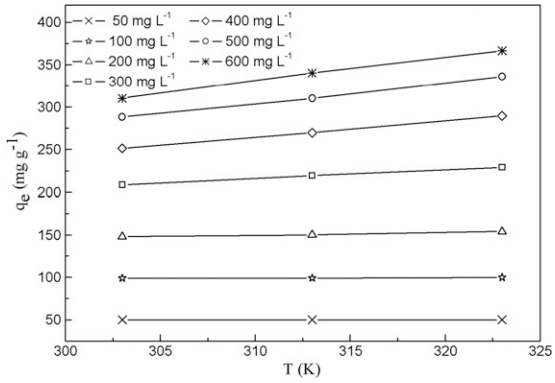

Figure 4. Effect of temperature on adsorption equilibrium at various initial methylene blue concentrations.

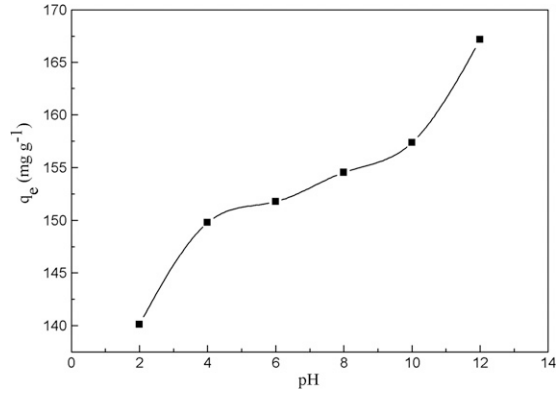

Figure 5. Effect of pH on the adsorption equilibrium of methylene blue onto windmill palm sheath fiber powder-based activated carbon.

initial concentration of the dye can enhance the adsorption process.

Effect of Temperature on Adsorption

Figure 4 shows the adsorption equilibrium (q_e) vs temperature at various initial MB concentrations (50-600 mg/L). Temperature had nearly no effect on the adsorption equilibrium when the MB concentration was lower (50-200 mg/L) and a significant effect when concentration was higher (300-600 mg/L). This indicates the endothermic nature of the adsorption reaction. This may be a result of the increase in the dye mobility with increasing temperature. Increasing temperature leads to an increase in the diffusion rate of the adsorbate molecules across the external boundary layer and in the internal pores of the adsorbent particle, thus owing to the decrease in the solution viscosity (Tan et al 2008b). An increasing number of MB molecules may also acquire sufficient energy to undergo an interaction with active sites on the surface (Hameed et al 2007a).

Effect of Solution pH on Adsorption

The effect of solution pH on the adsorption of MB onto WPFAC was studied at pH values of 2-12, a temperature of 40°C, and an initial dye concentration of 200 mg/L. pH affects the adsorption by influencing the chemistry of both dye molecules and the activated carbon in aqueous solution. Figure 5 shows the effect of solution pH on the adsorption of MB onto WPFAC. The adsorption of MB greatly depended on the solution pH, thus affecting the surface charge of the activated carbon and the ionization degree of the adsorbate. As shown in Fig 5, an increase in the solution pH from 2 to 12 enhanced the adsorption capacity (increased from 140.10 to 167.59 mg/g). At lower pH, more protons were available (excess H^+ ions), thus resulting in the protonation of MB in the acidic medium and the competition between dye cations and adsorption sites. However, at a higher pH, the abundance of OH^- ions increased the electrostatic attractions between the positively charged dye cations and negatively charged adsorption sites, thus increasing the dye uptake (Batzias and Sidiras 2007).

Adsorption Isotherm

The adsorption isotherm indicates how adsorption molecules are distributed between the liquid phase and solid phase when the adsorption process reaches an equilibrium state. The adsorption equilibrium data obtained for WPFAC were fitted into three different isotherm models to match the most suitable model that can represent the adsorption process. The Langmuir (Langmuir 1918), Freundlich (Freundlich 1906), and Dubinin–Radushkevich (Dubinin and Radushkevich 1947)

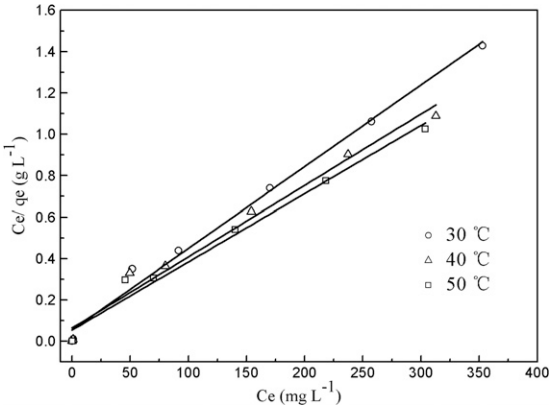

Figure 6. Langmuir isotherm for methylene blue adsorption onto windmill palm sheath fiber powder-based activated carbon at different temperatures.

equations are the most frequently used for describing adsorption isotherms.

Langmuir isotherm. The Langmuir isotherm assumes that adsorption occurs at specific homogeneous sites within the adsorbent without any interactions among the adsorbed substances. The linear form of the Langmuir isotherm model is given in Eq 3:

$$\frac{C_e}{q_e} = \frac{1}{q_{max}K_L} + \frac{C_e}{q_{max}} \quad (3)$$

where q_e is the solid-phase adsorbate concentration in equilibrium (mg/g), q_{max} is the maximum adsorption capacity that corresponds to complete monolayer coverage on the surface (mg/g), C_e is the concentration of adsorbate at equilibrium (mg/L), and K_L is the Langmuir constant related to adsorption rate (L/mg).

Figure 6 shows the slopes of the linear plots of C_e/q_e vs C_e. The Langmuir constants K_L and q_{max} were calculated from Eq 3. Their values are shown in Table 1.

Freundlich isotherm. The Freundlich equation is an empirical equation used to describe heterogeneous systems and is characterized by the heterogeneity factor $1/n$. Hence, a linear form of the Freundlich expression can be expressed as follows (Freundlich 1906):

$$\ln q_e = \ln K_F + \frac{1}{n}\ln C_e \quad (4)$$

where q_e is the solid-phase adsorbate concentration in equilibrium (mg/g), C_e is the equilibrium liquid-phase concentration (mg/L), K_F is the Freundlich constant (mg/g) $(L/mg)^{1/n}$, and $1/n$ is the heterogeneity factor.

Therefore, a plot of $\ln q_e$ vs $\ln C_e$ (Fig 7) enabled the constant K_F and exponent $1/n$ to be calculated and listed in Table 1. K_F and n are Freundlich constants, with n indicating the favorability of the adsorption process and K_F indicating the adsorption capacity of the adsorbent.

Dubinin–Radushkevich isotherm. Another popular equation for the analysis of isotherms with a high degree of rectangularity is the

Table 1. Langmuir, Freundlich, and Dubinin–Radushkevich isotherm model constants, separation factors (R_L), and correlation coefficients for adsorption of methylene blue on windmill palm sheath fiber powder-based activated carbon at 30°C, 40°C, and 50°C.

		Constants			
Isotherm model	Solution temperature (K)	q_{max} (mg/g)	K_L (L/mg)	R_L	R^2
Langmuir	303	253.16	0.07	0.02	0.99
	313	289.85	0.05	0.03	0.98
	323	303.95	0.06	0.03	0.98
Freundlich	Solution temperature (K)	K_F ([mg/g] $[L/mg]^{1/n}$)	$1/n$		R^2
	303	87.72	0.18		0.98
	313	83.61	0.21		0.95
	323	97.52	0.19		0.90
Dubinin–Radushkevich	Solution temperature (K)	q_s (mg/g)	E		R^2
	303	189.43	4.44×10^3		0.67
	313	206.44	0.99×10^3		0.70
	323	237.46	1.14×10^3		0.87

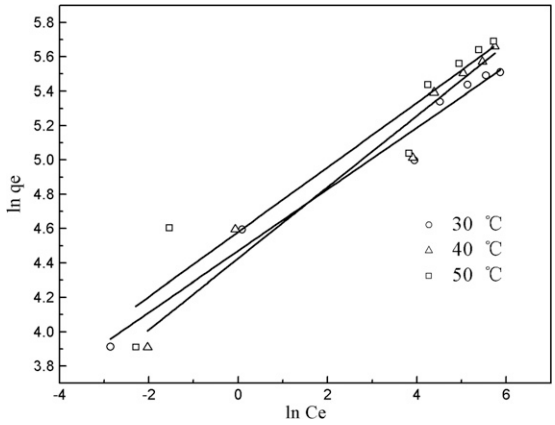

Figure 7. Freundlich isotherm for methylene blue adsorption onto windmill palm sheath fiber powder-based activated carbon at different temperatures.

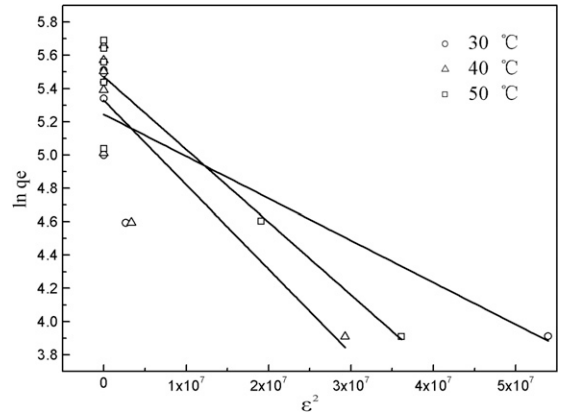

Figure 8. Dubinin–Radushkevich isotherm for methylene blue adsorption onto windmill palm sheath fiber powder-based activated carbon at different temperatures.

Dubinin–Radushkevich isotherm, which is expressed as follows:

$$q_e = q_s \exp(-B\varepsilon^2) \quad (5)$$

where ε can be correlated as follows:

$$\varepsilon = RT \ln\left(1 + \frac{1}{C_e}\right) \quad (6)$$

The constant B provides the mean free energy E of the sorption per molecule of the sorbate when it is transferred to the surface of the solid from infinity in the solution and can be computed using the following relationship:

$$E = \frac{1}{\sqrt{2B}} \quad (7)$$

where R is the gas constant (8.314 J/mol/K), and T (K) is the absolute temperature. The linearized form of Eq 5 is given as follows:

$$\ln q_e = \ln q_s - B\varepsilon^2 \quad (8)$$

A plot of ln q_e vs ε^2 (Fig 8) enabled the constants q_s and E to be determined.

As shown in Table 1, the Langmuir model yielded the best fit at all temperatures because its R^2 values were relatively higher than those of the other two isotherm models. The R_L value was 0.02-0.03, thus confirming that the Langmuir isotherm was favorable for the adsorption of MB on WPFAC under the conditions used in this study. For the Freundlich isotherm model, the $1/n$ values obtained for the WPFAC at all three temperatures studied were below one. This result demonstrated that the adsorption process followed a normal Langmuir isotherm. The conformation of the experimental data into Langmuir isotherm equation indicated the homogeneous nature of the surfaces of the activated carbon. The results also demonstrated the formation of the monolayer coverage of the dye molecule at the outer surfaces of the WPFAC. The adsorption behavior observed was predominantly monolayer adsorption, which involved chemical and physical adsorption. Literature has also indicated similar observations that the adsorption of MB on activated carbon was well represented by the Langmuir isotherm, such as the adsorption of MB on activated carbons prepared from oil palm fiber (Tan et al 2007), rattan sawdust (Hameed et al 2007b), and coconut husk (Tan et al 2008c).

Table 2 presents the comparison of the maximum monolayer adsorption capacity of MB onto activated carbon prepared from various precursors. The activated carbon prepared in this work had a relatively large adsorption capacity of 303.95 mg/g compared with some other adsorbents reported in literature. Therefore, the WPFAC prepared in this work could be used as an effective adsorbent for removing MB from aqueous solutions.

Table 2. Comparison of maximum monolayer adsorption of methylene blue dye onto activated carbon prepared from various precursors.

Precursor	Maximum monolayer adsorption capacity (mg/g)	References
Jute fiber	225.64	(Senthilkumaar et al 2005)
Oil palm shell	243.9	(Tan et al 2008a)
Oil palm fiber	277.78	(Tan et al 2007)
Rattan sawdust	294.14	(Hameed et al 2007b)
Palm kernel fiber	95.4	(EI-Sayed 2011)
Kenaf fiber char	18.18	(Mahmoud et al 2012)
Coir pith carbon	5.87	(Kavitha and Namasivayam 2007)
Sunflower oil cake	10.21-16.43	(Karagöz et al 2008)
Natural palygorskite	158.03	(Yenisoy-Karakas et al 2004)
Bamboo dust	143.2	(Bestani et al 2008)
Bituminous coal on a pilot scale	233-345	(El Qada et al 2008)
Commercial activated carbon	14	(Zhang et al 2015b)
Merck commercial activated carbon	200	(Kannan and Sundaram 2001)
WPFAC[a]	303.95	This work

[a] WPFAC, windmill palm sheath fiber powder-based activated carbon.

Adsorption Kinetics

The adsorption of dyes from the liquid phase to the solid phase can be considered a reversible reaction with equilibrium established between the two phases. To study the mechanism of MB adsorption on activated WPF, the pseudo-first-order, pseudo-second-order, and intraparticle diffusion equations were used to determine the adsorption mechanism.

Pseudo-first-order kinetic model. The pseudo-first-order equation given by Lagergren and Svenska (Ho and McKay 1998) is expressed as follows:

$$\ln (q_e - q_t) = \ln q_e - k_1 t \qquad (9)$$

where k_1 is the rate constant of the pseudo-first-order adsorption; q_e and q_t are the amounts of MB adsorbed (mg/g) at equilibrium and at time t (h), respectively. The values of k_1 were obtained from the slopes of the linear plots of ln $(q_e - q_t)$ vs t (Fig 9). The k_1 values, correlation coefficients R^2, and the experimental q_e ($q_{e,exp}$) and calculated q_e ($q_{e,cal}$) values are given in Table 3.

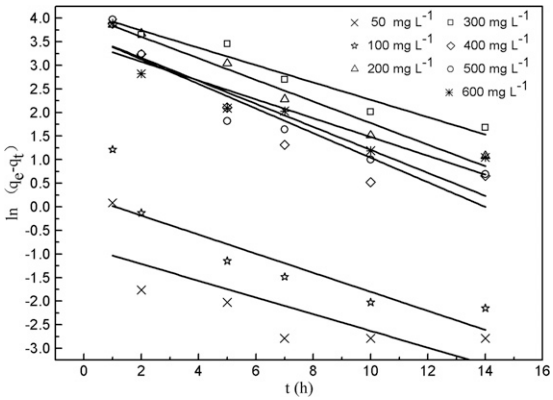

Figure 9. Pseudo-first-order kinetic model for adsorption of methylene blue on windmill palm sheath fiber powder-based activated carbon at 30°C.

Pseudo-second-order kinetic model. The pseudo-second-order model can be represented in the following form:

$$\frac{t}{q_t} = \frac{1}{k_2 q_e^2} + \frac{t}{q_e} \qquad (10)$$

where k_2 (h g/mg) is the rate constant for the pseudo-second-order adsorption kinetics. Figure 10 shows the pseudo-second-order plots of t/q_t vs t for MB onto WPFAC at 30°C. If the second-order kinetics are applicable, the plot should show a linear relationship. The slopes and intercepts of the plots enabled the values of q_e and k_2 to be calculated. The k_2, calculated q_e ($q_{e,cal}$), and correlation coefficient R^2 values are given in Table 3. The $q_{e,cal}$ values agreed with the $q_{e,exp}$ values, and the correlation coefficients for the pseudo-second-order kinetic plots at all studied concentrations

Table 3. Comparison of the pseudo-first-order, pseudo-second-order, and intraparticle diffusion models for adsorption of methylene blue (MB) on windmill palm sheath fiber powder-based activated carbon at 30°C.

Initial MB concentration (mg/L)	$q_{e,exp}$ (mg/g)	Pseudo-first-order kinetic model				Pseudo-second-order kinetic model				Intraparticle diffusion model			
		$q_{e,cal}$ (mg/g)	k_1 (h^{-1})	R^2	Δq_e (%)	$q_{e,cal}$ (mg/g)	k_2 (g/mg·h)	R^2	Δq_e (%)	$q_{e,cal}$ (mg/g)	K_p (mg/g·$h^{1/2}$)	R^2	Δq_e (%)
50	50	0.43	0.18	0.513	40.47	50	1.51	1.000	0	49.96	0.28	0.394	0.03
100	98.94	1.25	0.2	0.578	40.31	100	0.39	1.000	0.03	98.87	0.96	0.512	0.03
200	152.66	58.56	0.23	0.967	25.16	157.23	0.01	0.999	1.22	152.08	17.63	0.93	0.16
300	215.98	66.02	0.18	0.947	28.35	217.39	0.01	0.998	0.27	204.88	17.62	0.929	2.10
400	231.5	38.47	0.26	0.832	34.04	234.74	0.02	1.000	0.57	229.35	16.13	0.739	0.38
500	245.3	38.09	0.24	0.843	34.48	248.14	0.02	1.000	0.47	242.98	16.92	0.693	0.39
600	250.38	32.46	0.2	0.819	35.53	251.26	0.02	1.000	0.14	246.91	14.04	0.600	0.57

were higher than 0.999, thereby indicating the applicability of this model to describe the adsorption process of MB onto WPFAC.

Intraparticle Diffusion Model

Adsorption is a multistep process that involves the transport of solute molecules from the aqueous phase to the surface of the solid particulates, followed by diffusion into the interior of the pores. The intraparticle diffusion model was used to identify the diffusion mechanism, which was based on the theory proposed by Weber and Morris. This theory states the following:

$$q_t = k_p t^{1/2} \tag{11}$$

where k_p (mg/g $h^{1/2}$) is the intraparticle diffusion rate constant obtained from the slope of the straight line of q_t vs $t^{1/2}$ (Fig 11). The values of k_p, $q_{e,cal}$, and R^2 are listed in Table 3. If the intraparticle diffusion is rate limited, then the plot passed through the origin. As shown in Fig 11, the plots were nonlinear across the entire time range, thereby implying that more than one process affected the adsorption. At high initial concentrations (400, 500, and 600 mg/L), the diffusion model had two steps. The first one, the sharper portion, is the instantaneous adsorption or external surface adsorption. The second one is the gradual adsorption stage, in which intraparticle diffusion is rate limiting. The plots did not pass through the origin, and this deviation from the origin or near saturation might be caused by the difference in the mass transfer rate in the initial and final stages of adsorption (Mohanty et al 2005). These results showed that intraparticle diffusion was not the dominating mechanism for MB adsorption.

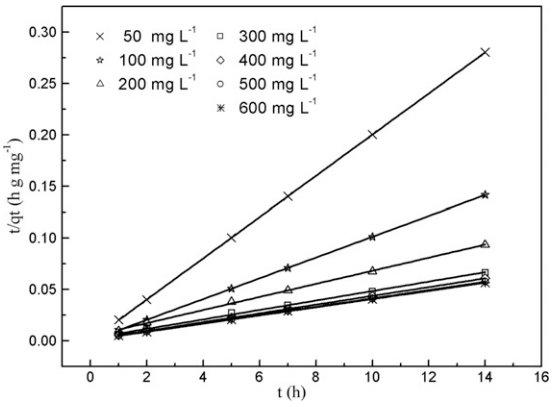

Figure 10. Pseudo-second-order kinetic model for adsorption of methylene blue on windmill palm sheath fiber powder-based activated carbon at 30°C.

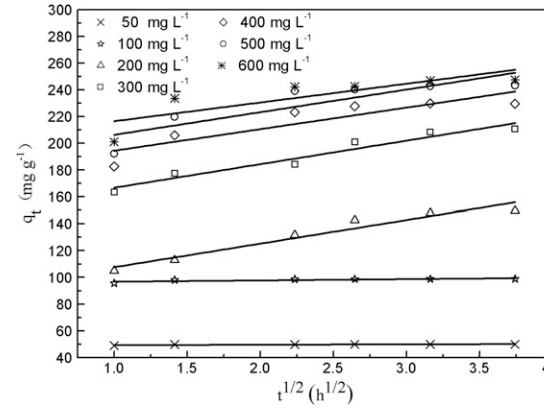

Figure 11. Intraparticle diffusion model for adsorption of methylene blue on windmill palm sheath fiber powder-based activated carbon at 30°C.

Normalized standard deviation Δq_e (%) was used to find the most applicable model that could describe the kinetic study of MB adsorption on WPFAC. The normalized standard deviation Δq_e (%) was calculated using the following equation:

$$\Delta q_e\ (\%) = 100 \times \left\{ \frac{\sum \left[\left(q_{e,exp} - q_{e,cal} \right) / q_{e,exp} \right]^2}{N-1} \right\}^{1/2} \quad (12)$$

where N is the number of data points. A low value of Δq_e (%) indicates a good fit.

According to Table 3, the pseudo-second-order and intraparticle diffusion kinetic models were found to provide low Δq_e (%) values of less than 1.2% and 2.1%, respectively, compared with 40.4% for the pseudo-first-order model. The suitability of the model for describing the adsorption kinetics was justified on the basis of the R^2 value. The R^2 values of the pseudo-second-order model for all MB concentrations, which were greater than 0.999, were obviously greater than those of the other two kinetic models. Therefore, the adsorption of MB onto WPFAC could be best described by the pseudo-second-order kinetic model based on equilibrium chemical adsorption, which predicted the behavior across the entire range of studies, strongly supported the model validity, and agreed with chemisorption being rate controlling (Tseng and Tseng 2005). Similar observations were found in literature (Wang and Zhu 2007), which have concluded that the adsorption kinetics of MB on activated carbons obeyed the pseudo-second-order kinetic model.

Adsorption Thermodynamics

The concept of thermodynamics assumes that in an isolated system wherein energy cannot be gained or lost, entropy change is the driving force (Kumar and Kumaran 2005). The thermodynamic behavior of the adsorption of MB on WPFAC was evaluated by thermodynamic parameters, including changes in standard enthalpy (ΔH^0), standard entropy (ΔS^0), and standard free energy (ΔG^0). The values of ΔH^0 and ΔS^0 were computed using the following equation:

$$\ln k_d = \frac{\Delta S^0}{R} - \frac{\Delta H^0}{RT} \quad (13)$$

where R (8.314 J/mol/K) is the universal gas constant, T (K) is the absolute solution temperature, and K_d is the distribution coefficient. K_d can be calculated as follows:

$$k_d = \frac{C_{Ae}}{C_e} \quad (14)$$

where C_{Ae} (mg/L) is the amount adsorbed on solid at equilibrium and C_e (mg/L) is the equilibrium concentration. The values of ΔH^0 and ΔS^0 were calculated from the slope and intercept of the van't Hoff plots of $\ln K_d$ vs $1/T$ (Fig 12). ΔG^0 can be calculated using the relation below:

$$\Delta G^0 = -RT \ln k_d \quad (15)$$

The calculated values of ΔH^0, ΔS^0, and ΔG^0 are listed in Table 4. The negative values of ΔG^0 indicated the feasibility of the adsorption process and the thermodynamically spontaneous nature of the adsorption with a strong preference of MB onto WPFAC. The positive values of ΔH^0 indicated the endothermic nature of the adsorption interaction. This result agreed with and further confirmed the maximum monolayer adsorption

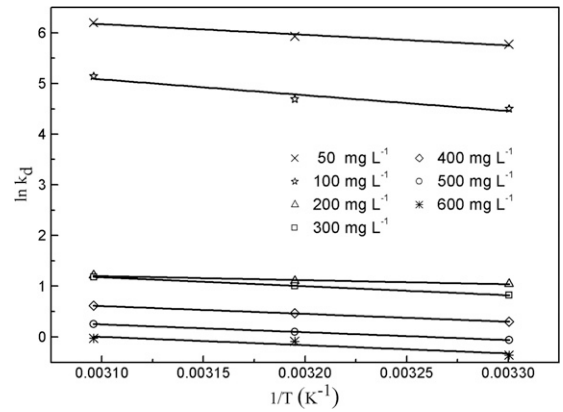

Figure 12. Plot of $\ln k_d$ vs $1/T$ at various initial methylene blue concentrations.

Table 4. Thermodynamic parameters for adsorption of methylene blue onto windmill palm sheath fiber powder-based activated carbon.

Initial concentration (mg/L)	$\triangle H^0$ (J/mol)	$\triangle S^0$ (J/mol/K)	$\triangle G^0$ (J/mol)		
			303 K	313 K	323 K
50	17,337.98	105.05	−14,492.26	−15,542.76	−16,593.26
100	25,887.52	122.51	−11,232.56	−12,457.65	−13,682.73
200	6,695.46	30.74	−2,618.60	−2,925.95	−3,233.35
300	14,759.90	55.55	−2,071.00	−2,626.47	−3,181.94
400	12,842.39	47.72	−1,615.50	−2,092.65	−2,569.81
500	12,802.14	45.08	−857.15	−1,307.95	−1,758.75
600	13,584.64	44.93	−30.82	−480.18	−929.53

capacity of MB onto WPFAC, which increased from 253.16 to 303.95 mg/g as solution temperature increased from 30°C to 50°C (Table 1). The endothermic processes of the adsorption reaction might have been caused by the temperature increase, which sped up the diffusion rate of the adsorbate molecules across the external boundary layer and in the internal pores of the adsorbent particle owing to the decrease in the solution viscosity. The positive value of $\triangle S^0$ suggested an increased disorder at the solid–solution interface and affinity of WPFAC for MB during the adsorption process.

CONCLUSIONS

In this study, we investigated the porous features of WPFAC. We also studied absorption performances on MB and its absorption isotherms, kinetics, and thermodynamics using the equilibrium data. The nitrogen adsorption isotherm corresponded to the intermediate between types I and II under the IUPAC classification. It also showed a combination of microporous and mesoporous structure of WPFAC with BET surface of 1049.26 m^2/g, which indicated that WPFAC has a significant adsorption capacity. The investigation of the effect parameters indicated that the adsorption of MB increased with increasing contact time, MB initial concentration, and solution temperature. Alkaline solution pH was proven to be favorable for the adsorption of MB on WPFAC.

The equilibrium data were best represented by the Langmuir isotherm. The maximum monolayer adsorption capacity of MB onto WPFAC increased from 253.16 to 303.95 mg/g with an increase of solution temperature from 30°C to 50°C. The excellent adsorbing performance illustrated that its maximum monolayer adsorption capacity was up to 51.78 times higher than other absorbents. The adsorption kinetics closely followed the pseudo-second-order kinetic model, which provided the lowest $\triangle q_e$ % (1.2%) and the greatest R^2 values (0.999). The positive $\triangle H^0$ and negative $\triangle G^0$ values indicated the endothermic and spontaneous process of the adsorption of MB onto WPFAC. The positive $\triangle S^0$ values showed increased randomness at the solid–solution interface during the adsorption process. WPFAC is a promising adsorbent and could be of great potential value for use as a new agricultural resource for its amazing adsorption capacity.

ACKNOWLEDGMENTS

We acknowledge the research grant provided by the Postgraduates' Scientific Research Innovation Project in Chongqing (CYB14057) and the Fundamental Research Funds for the Central Universities (XDJK2016E045, XDJK2015D006, XDJK2013A021).

REFERENCES

Ahmad AA, Hameed BH, Aziz N (2007) Adsorption of direct dye on palm ash: Kinetic and equilibrium modeling. J Hazard Mater 141:70-76.

Batzias FA, Sidiras DK (2007) Adsorption by prehydrolised beech sawdust in batch and fixed-bed systems. Biores Technol 98:1208-1217.

Bestani B, Benderdouche N, Benstaali B, Belhakem M, Addou A (2008) Methylene blue and iodine adsorption onto an activated desert plant. Biores Technol 99:8441-8444.

Brunauer S, Emmet PH, Teller F (1938) Adsorption of gases in multimolecular layers. J Am Chem Soc 60:309-319.

Cheng L, Zhang TH, Guo M, Li XL (2014) Structural characteristics and properties of windmill palm leaf sheath fiber. Wood Fiber Sci 46(2):270-279.

Dubinin MM, Radushkevich LV (1947) Equation of the characteristic curve of activated charcoal. Proc Acad Sci Phys Chem Sec 331-333:875-890.

El Qada EN, Allen SJ, Walker GM (2008) Adsorption of basic dyes from aqueous solution onto activated carbon. Chem Eng J 135:174-184.

EI-Sayed GO (2011) Removal of methylene blue and crystal violet from aqueous solutions by palm kernel fiber. Desalination 272:225-232.

Fernandez ME, Nunell GV, Bonelli PR, Cukierman AL (2014) Activated carbon developed from orange peels: Batch and dynamic competitive adsorption of basic dyes. Ind Crops Prod 62:437-445.

Foo KY, Hameed BH (2011) Microwave-assisted preparation of oil palm fiber activated carbon for methylene blue adsorption. Chem Eng J 166:792-795.

Freundlich HMF (1906) Over the adsorption in solution. J Chem Phys 57:385 -470.

Guo M, Zhang TH, Chen BW, Cheng L (2014) Tensile strength analysis of palm leaf sheath fiber with Weibull distribution. Compos Part A-Appl S 62:45-51.

Hameed BH, Ahmad AA, Aziz N (2007a) Isotherms, kinetics and thermodynamics of acid dye adsorption on activated palm ash. Chem Eng J 133:195-203.

Hameed BH, Ahmad AA, Aziz N (2009) Adsorption of reactive dye on palm-oil industry waste: Equilibrium, kinetic and thermodynamic studies. Desalination 247:551-560.

Hameed BH, Ahmad AL, Latiff KNA (2007b) Adsorption of basic dye (methylene blue) onto activated carbon prepared from rattan sawdust. Dyes Pigments 75:143-149.

Ho YS, McKay G (1998) Sorption of dye from aqueous solution by peat. Chem Eng J 70:115-124.

Kannan N, Sundaram MM (2001) Kinetics and mechanism of removal of methylene blue by adsorption on various carbons—A comparative study. Dyes Pigments 51:25-40.

Karagöz S, Tay T, Ucar S, Erdem M (2008) Activated carbons from waste biomass by sulfuric acid activation and their use on methylene blue adsorption. Biores Technol 99:6214-6222.

Kavitha D, Namasivayam C (2007) Experimental and kinetic studies on methylene blue adsorption by coir pith carbon. Biores Technol 98:14-21.

Kumar KV, Kumaran A (2005) Removal of methylene blue by mango seed kernel powder. Biochem Eng J 27:83-93.

Langmuir I (1918) The adsorption of gases on plane surfaces of glass, mica and platinum. J Am Chem Soc 40:1361-1403.

Liu XH, Yang YL, Shi XX, Li KX (2015) Fast photocatalytic degradation of methylene blue dye using a low-power diode laser. J Hazard Mater 283:267-275.

Maatar W, Alila S, Boufi S (2013) Cellulose based organogel as an adsorbent for dissolved organic compounds. Ind Crops Prod 49:33-42.

Macías-García A, Cuerda-Correa EM, Olivares-Marín M, Díaz-Paralejo A, Díaz-Díez MA (2012) Development and characterization of carbon-honeycomb monoliths from kenaf natural fibers: A preliminary study. Ind Crops Prod 35:105-110.

Mahmoud DK, Salleh MAM, Karim WAWA, Idris A, Abidin ZZ (2012) Batch adsorption of basic dye using acid treated kenaf fibre char: Equilibrium, kinetic and thermodynamic studies. Chem Eng J 181-182:449-457.

Martin MJ, Artola A, Balaguer MD, Rigola M (2003) Activated carbons developed from surplus sewage sludge for the removal of dyes from dilute aqueous solutions. Chem Eng J 94:231-239.

Mohanty K, Das D, Biswas MN (2005) Adsorption of phenol from aqueous solutions using activated carbons prepared from Tectona grandis sawdust by $ZnCl_2$ activation. Chem Eng J 115:121-131.

Senthilkumaar S, Varadarajan PR, Porkodi K, Subbhuraam CV (2005) Adsorption of methylene blue onto jute fiber carbon: Kinetics and equilibrium studies. J Colloid Interface Sci 284:78-82.

Tan IAW, Ahmad AL, Hameed BH (2008a) Adsorption of basic dye using activated carbon prepared from oil palm shell: Batch and fixed bed studies. Desalination 225:13-28.

Tan IAW, Ahmad AL, Hameed BH (2008b) Enhancement of basic dye adsorption uptake from aqueous solutions using chemically modified oil palm shell activated carbon. Colloid Surface A 318:88-96.

Tan IAW, Ahmad AL, Hameed BH (2009) Adsorption isotherms, kinetics, thermodynamics and desorption studies of 2,4,6-trichlorophenol on oil palm empty fruit bunch-based activated carbon. J Hazard Mater 164:473-482.

Tan IAW, Hameed BH, Ahmad AL (2007) Equilibrium and kinetic studies on basic dye adsorption by oil palm fibre activated carbon. Chem Eng J 127:111-119.

Tan IAW, Hameed BH, Ahmad AL (2008c) Optimization of preparation conditions for activated carbons from coconut husk using response surface methodology. Chem Eng J 137:462-470.

Treviño-Cordero H, Juárez-Aguilar LG, Mendoza-Castillo DI, Hernández-Montoya V, Bonilla-Petriciolet A, Montes-Morán MA (2013) Synthesis and adsorption properties of activated carbons from biomass of *Prunus domestica* and *Jacaranda mimosifolia* for the removal of heavy metals and dyes from water. Ind Crops Prod 42:315-323.

Tseng RL, Tseng SK (2005) Pore structure and adsorption performance of the KOH-activated carbons prepared from corncob. J Colloid Interface Sci 287:428-437.

Vieira SS, Magriotis ZM, Santos, NAV, Cardoso, M das Gracas, Saczk AA (2012) Macauba palm (*Acrocomia aculeata*) cake from biodiesel processing: An efficient and low cost substrate for the adsorption of dyes. Chem Eng J 183:152-161.

Wang S, Zhu ZH (2007) Effects of acidic treatment of activated carbons on dye adsorption. Dyes Pigments 75:306-314.

Yenisoy-Karakas S, Aygün A, Günes M, Tahtasakal E (2004) Physical and chemical characteristics of polymer-based spherical activated carbon and its ability to adsorb organics. Carbon 42:477-484.

Zhang TH, Guo M, Cheng L, Li XL (2015a) Investigations on the structure and properties of palm leaf sheath fiber. Cellulose 22(2):1039-1051.

Zhang Y, Wang WB, Zhang JP, Liu P, Wang AQ (2015b) A comparative study about adsorption of natural palygorskite for methylene blue. Chem Eng J 262:390-398.